ISBN: 978-3-95450-212-7 ISSN: 2673-5482 doi:10.18429/JACoW-CYCLOTRONS2022-THPO003

APPLICATIONS OF THE CYCIAE-100 CYCLOTRON IN NEUTRON-INDUCED SINGLE EVENT EFFECT

Q. M. Chen, J. Bao, G. Guo*, J. H. Han, X. Ma, S. Y. Zhao
China Institute of Atomic Energy, Beijing, China
National Innovation Center of Radiation Application, Beijing, China

Abstract

Neutron-induced single event effect is one of the significant factors affecting the reliability of semiconductor devices in avionics and ground facilities. The 100 MeV proton cyclotron in China Institute of Atomic Energy (CYCIAE-100) provides white neutron and quasi-monoenergetic neutron induced by proton and W/Li bombardment. Based on the white neutron beam of CYCIAE-100, the white neutron energy spectrum was measured by neutron time-of-flight method with double scintillator spectrometer, as well as the theoretical energy spectrum was calculated by the Monte Carlo method. The neutron irradiation test for ESA SEU monitor with different technology nodes were carried out, and the neutron single event upset sections are obtained simultaneously. In addition, based on the quasi-monoenergetic neutron beam line, the simulation of neutron energy spectrum was carried out. As a conclusion, the white neutron and quasi-monoenergetic neutron provided by CYCIAE-100 are well suitable applied to the study of neutron single event effects.

INTRODUCTION

Galactic cosmic rays and solar rays interact with nitrogen and oxygen in the earth's atmosphere to produce a large number of neutrons. Neutron incident semiconductor devices cause single event effects (SEEs), leading to logic inversion and functional failure, which seriously threaten the safety and reliability of aircraft electronic systems [1-3]. In addition, in the nuclear power stations and spent fuel reprocessing plants, neutron radiation produced by the nuclear reaction also reduce the reliability of electronic control systems and visual monitoring systems.

In order to measure the neutron-induced single event effects and to evaluate the risks of neutron radiation, accelerated tests based on the ground neutron sources were performed and progressively became the predominant approach, since the environmental atmospheric neutron test is time-consuming. Many neutron irradiation test equipment from white neutron source, quasi-monoenergetic neutron source and 14 MeV monoenergetic neutron source has been established, such as CHIPIR of ISIS [4], QMN of TSL [5], and so on. The white neutron source, which has an energy spectrum very close to the atmosphere neutron environment, are used to directly evaluate the atmospheric neutron effect. As a contrast, the monoenergetic and quasi-monoenergetic neutron sources are used to measure the cross-section curve of SEEs as a function of neutron energy, which is helpful in exploring the mechanism of the neutron SEEs.

* ggg@ciae.ac.cn.

In 2016, the first SEE experiment for electronic devices was carried out on the 100 MeV proton cyclotron (CYCIAE-100) in China Institute of Atomic energy (CIAE). This cyclotron provides a 70–100 MeV, 0.01-200 μA proton beam [6]. Meanwhile, with W and Li targets, both white neutron and quasi-monoenergetic neutron can be produced by proton and W/Li bombardment, which provides good neutron sources for experimental research of neutron SEEs.

In this paper, we first measured the white neutron energy spectrum by time-of-flight method with double scintillator, and then tested neutron SEE for ESA SEU monitor. The possibility and ability of irradiation test by quasi-monoenergetic neutron were also analysed.

WHITE NEUTRON EXPERIMENT

Prior to SEE testing, the neutron energy spectrum shall be accurately measured. Since the CYCIAE-100 induces a continuous proton beam, the withe neutron beam produced by proton bombards W targets is also a continuous beam. The conventional neutron measurement methods for pulsed neutron are not adequate. Therefore, the neutron time-of-flight (TOF) experiment with two scintillator detectors were performed. By measuring the neutron flight time at a certain distance, we obtain the flight speed of neutrons, and hence the energy of neutrons.

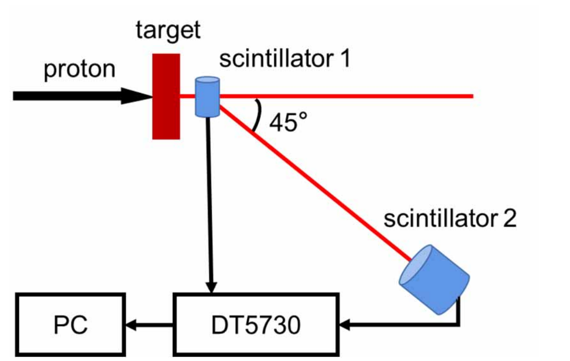

Figure 1: The measurement of white neutron spectrum.

The white neutron target is tungsten copper alloy WCu7, 93% of which is tungsten, 12 mm thickness and 75 mm diameter. After passing through 2 mm copper and 5 mm water, 100 MeV protons bombard the 12 mm thick WCu7 target and white neutron are produced.

As shown in Fig. 1, one liquid scintillator detector (scattering detector) is placed on the neutron beam behind the target, which is detect the start signal of flight neutron, and the other (main detector with high efficiency) is placed at a distance L (L=3 m) and 45° direction of the proton beam, which is detected the stop signal of flight neutron. The

ISBN: 978-3-95450-212-7 ISSN: 2673-5482 doi:10.18429/JACoW-CYCLOTRONS2022-THPO003

gamma signal was removed by pulse shape discrimination (PSD), and the time spectrum of flight neutron were acquired by a DT5730 digitizer in the coincidence mode, see Fig. 2.

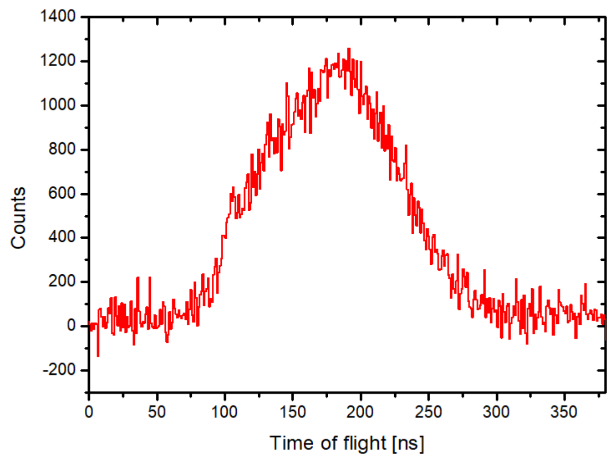

Figure 2: The TOF spectrum of white neutron spectrum.

With the detection efficiency correction for two liquid scintillators by Monte Carlo simulation, the neutronic energy spectrum can be obtained by converting the TOF spectrum with Eq. (1).

$$E = m_0 c^2 \left(\frac{1}{\sqrt{1-(\frac{L}{tc})^2}} - 1 \right) \tag{1}$$

where E is the energy of flight neutron, m_0 is the mass of neutron, L is the distance between two scintillator detectors, t is the flight time of neutron and c is the velocity of light.

Figure 3 shows the measured neutron energy spectrum and contrasts it with the theoretical spectrum simulated by Monte Carlo method. Limited by the need to discriminate against gamma rays, the lower limit energy of the neutron measured is only 3 MeV, the Fig. 3 showed that the measured energy spectrum almost completely coincided with the calculated one from 3 MeV to 100 MeV energy region.

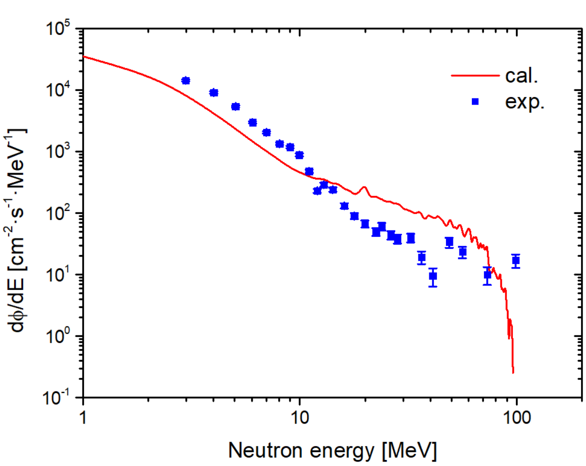

Figure 3: The measured energy spectrum, and compare to the theoretical spectrum by Monte Carlo simulation.

As a result, with 100 MeV/1 μA proton, 3.28×10^4 n/(cm^2·s) neutron from 3 MeV to 100 MeV were produced at the position 15 m away from the target in 0-degree direction, and neutrons above 10 MeV account for 12.4%.

Base on the white neutron spectrum, the Europe space agency single event upset monitor (ESA SEU Monitor) was applied to measure the cross section of neutron SEU.

The irradiation experimental results show that the neutron SEU cross section of the SEU Monitor (250 nm, 16 Mbit, 3.3 V) is 31.0 upsets/h with 3 μA proton, that is 5.47×10^{-15} upsets/(cm^2·bit). Usually, 10 MeV is considered as a threshold energy for high energy neutron SEE, but more and more evidences are provided to certify that less energy neutron can also lead to SEE in advanced electronic systems [7, 8]. The contribution of neutron below 10 MeV to SEE is critical too. Considering the energy above 10 MeV accounts for 12.4% of the white neutron source in CYCIAE-100, this neutron source is more suitable to test the neutron radiation effects for nuclear industry rather than for atmospheric environment.

QUASI-MONOENERGETIC NEUTRON SIMULATION

The monoenergetic neutron in the energy range of several MeV to 20 MeV are mainly produced by the two-body nuclear reaction induced by different light ions, such as the 14 MeV D-T neutron source. In the energy region above 20 MeV, ^{7}Li (p, n) ^{7}Be reactions are primary used.

The reaction energy of ^{7}Li (p, n)^{7}Be is -1.646 MeV and the threshold energy of neutron production is 1.881 MeV. At the incident proton energy of 1.9-2.4 MeV, the ^{7}Li (p, n)^{7}Be reaction produces only the ground state ^{7}Be, i. e., ^{7}Li (p, n_0)^{7}Be, and the produced neutrons are monoenergetic neutrons with a large cross section (300-500 mb). The proton energy exceeds 2.4 MeV and the produced ^{7}Be can be excited to its first excited state (0.43 MeV), i.e., ^{7}Li (p, n_0)^{7}Be and ^{7}Li (p, n_1)^{7}Be occur simultaneously. For SEE cross-sections, the energy dependence is not particularly sensitive, so both n_0 and n_1 are treated as single-energy peak neutrons. When the proton energy exceeds 3.68 MeV, the ^{7}Li (p, n^{3}He)^{4}He reaction channel is opened, which is a three-body reaction and produces neutrons as a continuum spectrum with energies below the monoenergetic peak. Higher proton energies even excite ^{7}Be to the second and third excited states as well as other multi-body breakup reaction. In summary, n_0 and n_1 from ^{7}Li (p, n_0)^{7}Be and ^{7}Li (p, n_1)^{7}Be constitute the monoenergetic peak neutron, while neutrons from other reaction channels constitute the continuous spectrum of neutrons with lower energy than the monoenergetic peaks.

Since the ^{7}Li (p, $n_{0,1}$)^{7}Be reaction has the largest cross section in the 0° emission direction, the neutron from 0° emission direction is chosen as the irradiation source. Figure 4 shows the cross sections of the ^{7}Li (p, $n_{0,1}$)^{7}Be reaction at different energy proton from 10 MeV to 800 MeV, and it can be seen that the cross sections are first increasing rapidly and then then tends to be flat (data source [9, 10]), as shown in Fig. 4.

ISBN: 978-3-95450-212-7 ISSN: 2673-5482 doi:10.18429/JACoW-CYCLOTRONS2022-THPO003

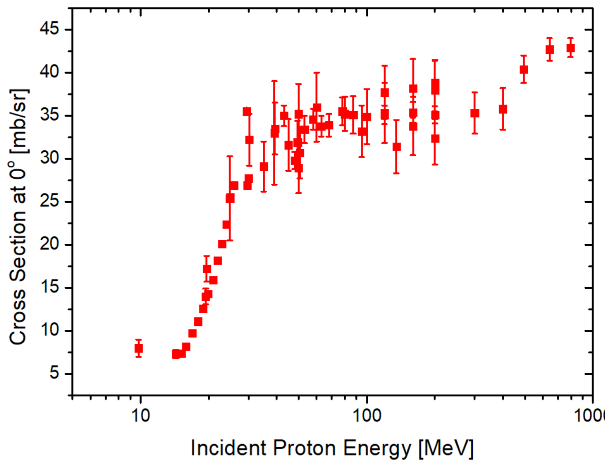

Figure 4: Nuclear reaction cross-section of ^{7}Li (p,n$_{0,1}$)^{7}Be.

The neutron flux of the monoenergetic peak emitted at the 0° direction can be calculated using the following equation

$$\Phi_{\theta=0}(n_{0,1}) = \sigma_{\theta=0}(n_{0,1}) \times \Phi_p \times \rho_{\,^7Li} \times d_{\,^7Li} \qquad (2)$$

where $\sigma_{\theta=0}(n_{0,1})$ is the 0° direction ^{7}Li (p, n$_{0,1}$)^{7}Be reaction cross section, Φ_p is the incident proton intensity, $\rho_{\,^7Li}$ is the atomic density of the ^{7}Li target, and $d_{\,^7Li}$ is the ^{7}Li target thickness.

For 100 MeV/1 μA incident protons, the neutron flux calculated by Eq. (2) is 1.28×10^4 n/(m^2·s) at a position 5 m away from the Li target.

In fact, the quasi-monoenergetic neutron target is natural Li, 6 mm thickness and 52 mm diameter. Figure 5 shows the theoretical spectrum by Monte Carlo simulation. With 100 MeV/1 μA proton, 2.92×10^4 n/(cm^2·s) neutron from 0 MeV to 100 MeV were produced at the position 5 m away from the target in 0 degree direction, and monoenergetic peak neutrons account for 51.8%. Since 70, 80, 90, 100 MeV protons can be derived from the CYCIAE-100 directly, so four quasi-monoenergetic neutron sources are available for neutron radiation effects.

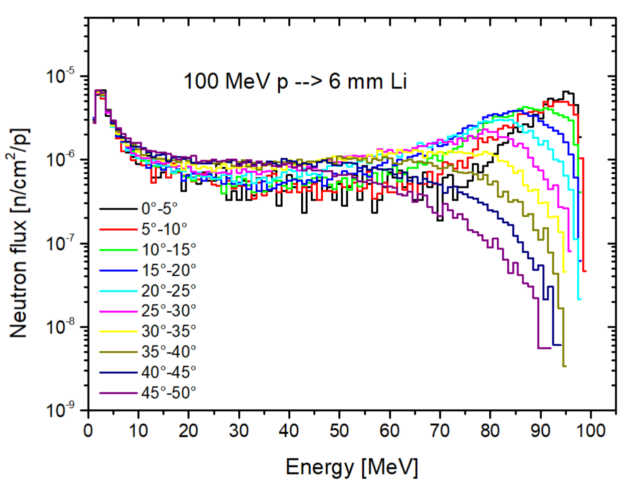

Figure 5: Neutron spectrum of 100 MeV proton bombards the 6 mm Li target.

As shown in Fig. 5, the neutron energy spectrum differs greatly in different emission directions, with the highest proportion of peak neutrons in the high-energy part of the 0-5 direction. The main reason is that the Li(p, n) reaction consists of direct nuclear reaction mechanism and compound nucleus reaction mechanism, the direct nuclear reaction is mainly the knockout reaction, which produces neutrons with foreshortening and high energy, while the compound nucleus reaction evaporation neutrons in all directions, which is homogeneity and is mainly low-energy neutrons. Therefore, the neutrons in the 0° emission direction have the best monochromaticity, which is used to carry out the irradiation text for neutron SEEs.

Because higher incident energy will lead to a multi-body breakup reaction, only quasi-monoenergetic neutrons can be obtained, thus their energy spectra contain not only monoenergetic peak fractions but also low-energy tail continuous fractions. These trailing neutrons can also trigger SEEs, which affect the accuracy of neutron SEEs cross section measurements. Nevertheless, since the quasi-monoenergetic neutron has a high proportion of monoenergetic peak neutrons, up to 40% or even higher, the SEEs due to low-energy neutrons can be corrected by the tail neutron correlation method and the accurate cross-section of neutron SEEs obtained.

CONCLUSION

The white neutron spectrum measurement and the first neutron single event effect test were performed based on the CYCIAE-100 cyclotron in CIAE. With 100 MeV/1 μA proton, 3.28×10^4 n/(cm^2·s) neutron provided to irradiate the electronics device. Considering the neutrons above 10 MeV account for 12.4%, the white neutron source is more suitable to test the neutron radiation effects for nuclear industry rather than for atmospheric environment. The quasi-monoenergetic neutron spectrum simulated by Monte Carlo method, with 100 MeV/1 μA proton, 2.92×10^4 n/(cm^2·s) neutron were provided to irradiate the electronics device. Since 70, 80, 90, 100 MeV protons can be derived from the CYCIAE-100 directly, so four quasi-monoenergetic neutron sources are available for neutron radiation effects.

ACKNOWLEDGEMENTS

Valuable discussions with Dr. W. W. Qu of Soochow university are acknowledged. We are grateful to the CYCIAE-100 cyclotron staff for the operation of the machine.

REFERENCES

[1] E. Normand, “Single-event effects in avionics”, *IEEE Trans. Nucl. Sci.*, vol. 43, pp. 461-473, 1996. doi:10.1109/23.490893

[2] C. Dyer *et al.*, “Testing Across a Wide Range of Energies and Facilities and Implications for Standards”, *IEEE Trans. Nucl. Sci.*, vol. 53, pp. 3596-3601, 2006. doi:10.1109/TNS.2006.886207

[3] P. Ramos *et al.*, “Evaluating the SEE sensitivity of a 45nm SOI multi-core processor due to 14 MeV neutrons”, *IEEE*

ISBN: 978-3-95450-212-7 ISSN: 2673-5482 doi:10.18429/JACoW-CYCLOTRONS2022-THPO003

Trans. Nucl. Sci., vol. 63, pp. 2193-2200, 2016. doi:10.1109/TNS.2016.2537643

[4] C. Andreani *et al.*, "Facility for fast neutron irradiation tests of electronics at the ISIS spallation neutron source", *Appl. Phys. Lett.*, vol. 92, pp. 114101, 2008. doi:10.1063/1.28973

[5] V. Alexander *et al.*, "CUP–A New High-Flux Irradiation Position at the ANITA Neutron Facility at TSL", *IEEE Trans. Nucl. Sci.*, vol. 61, pp. 1929-1936, 2014. doi:10.1109/TNS.2014.2319098

[6] E. Ibe *et al.*, "An automatic phase matching technique of CYCIAE-100 cyclotron", *Nucl. Sci. Tech.*, vol. 28, pp. 1–6, 2017. doi:10.1007/s41365-017-0277-9

[7] J. L. Autran *et al.*, "Soft-error rate induced by thermal and low energy neutrons in 40 nm SRAMs", *IEEE Trans. Nucl. Sci.*, vol. 59, pp. 2658–2665, 2012. doi:10.1109/TNS.2012.2222438

[8] E. Ibe *et al.*, "Impact of scaling on neutron-induced soft error in SRAMs from a 250 nm to a 22 nm design rule", *IEEE Trans. Nucl. Sci.*, vol. 57, pp. 1527–1538, 2010. doi:10.1109/TED.2010.2047907

[9] H. Guo *et al.*, "Application of the continuum discretized coupled channels method to nucleon-induced Reactions on ^{6,7}Li for Energies up to 150 MeV", *Nucl. Data Sheets*, vol. 118, pp. 254–257, 2014. doi:10.1016/j.nds.2014.04.051

[10] Y. Iwamoto *et al.*, "Characterization of high-energy quasi-monoenergetic neutron energy spectra and ambient dose equivalents of 80-389 MeV ^{7}Li(p, n) reactions using a time-of-flight method", *Nucl. Instrum. Meth. Phys. Res. Sect. A*, vol. 804, pp. 50–58, 2015. doi:10.1016/j.nima.2015.09.045